

Assessing Urban Expansion and Inundation Risk in Hangzhou's Central Districts

Abstract

Urban flooding is a growing concern in rapidly urbanizing cities, where impervious surface expansion alters hydrological processes and increases flood vulnerability. This report examines the relationship between urban development and inundation risk in the central districts of Hangzhou, China, from 2018 to 2023. A two-stage geospatial framework is employed. First, impervious surfaces are detected using a UNet-based deep learning segmentation model applied to Sentinel-2 imagery. Second, inundation-prone zones are delineated using the Height Above Nearest Drainage (HAND) model adjusted by surface runoff potential. Spatial analysis reveals a marked increase in impervious cover, particularly in Yuhang and Xiaoshan Districts, and a corresponding expansion of high-risk inundation zones. The results highlight a strong spatial correlation between urban expansion and increased inundation risk, emphasizing the need for targeted flood mitigation strategies and sustainable land-use planning in rapidly growing urban regions.

1. Introduction

Urban flooding has become an increasingly critical issue amid the rapid expansion of impervious surfaces in cities. Hangzhou, a major city in eastern China, has experienced significant urbanization, particularly in its central districts including Linping District, Qiantang District, Yuhang District, Gongshu District, Shangcheng District, Xihu District, Binjiang District, and Xiaoshan District. These areas have seen extensive land-use changes and a sharp increase in impervious surfaces, contributing to greater inundation risks during heavy rainfall events. Understanding the spatial distribution of inundation-prone areas and the dynamics of impervious surface changes is essential for urban flood management and sustainable planning. By integrating DEM-based hydrological modeling and remote sensing analysis, this report aims to identify high-risk inundation areas and quantify the relationship between urban development and inundation vulnerability in the central Hangzhou.



Figure1: Study Area

Note: Administrative boundary data retrieved from TianDiTu (2024)¹.

¹ TianDiTu. (2024). Administrative Division Boundary Data. TianDiTu Cloud Center. <https://cloudcenter.tianditu.gov.cn/administrativeDivision>

2. Methodology

A two-stage geospatial analysis framework was developed to assess inundation risk and the impact of land cover changes in Hangzhou's urban core.

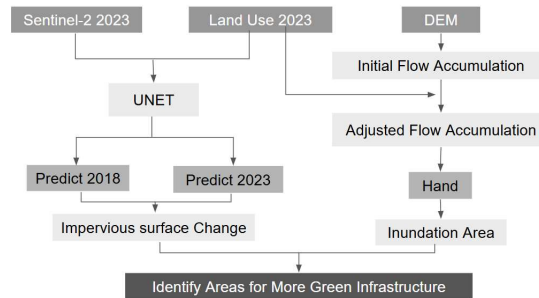


Figure 2: Workflow

2.1 Detect Impervious Surface Using UNet

To detect urban development, a UNet-based semantic segmentation model was employed to map impervious surfaces. The model was trained on the SinoLC-1 dataset² and Sentinel-2 Level-2A surface reflectance data³. Selected spectral bands used as input include B03 (Green), B04 (Red), B08 (Near-Infrared), and B11 (Shortwave Infrared), which are sensitive to built-up areas. The output includes three classes: impervious surface, pervious surface, and nodata. The prediction pixels show high accuracy to separate impervious surfaces with pervious surfaces.

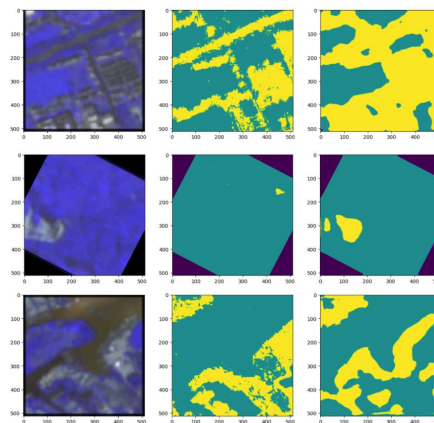


Figure 3: Predict using UNet-based Model

Note: From left to right – raw remote sensing image, initial label, and model prediction.

Predicted maps using the final model for 2018 and 2023 reveal urban expansion primarily towards north and east. Impervious surface coverage increased from 24.5% in 2018 to 40.8% in 2023, with the most significant growth observed in Yuhang and Xiaoshan Districts.

² Zhuohong Li, et al. (2023). SinoLC-1: A high-resolution (1 m) national-scale land cover product [Dataset]. Zenodo. <https://doi.org/10.5281/zenodo.7709370>

³ European Space Agency. (2024). Copernicus Sentinel-2 Level-2A Surface Reflectance Product. Google Earth Engine. https://developers.google.com/earth-engine/datasets/catalog/COPERNICUS_S2_SR

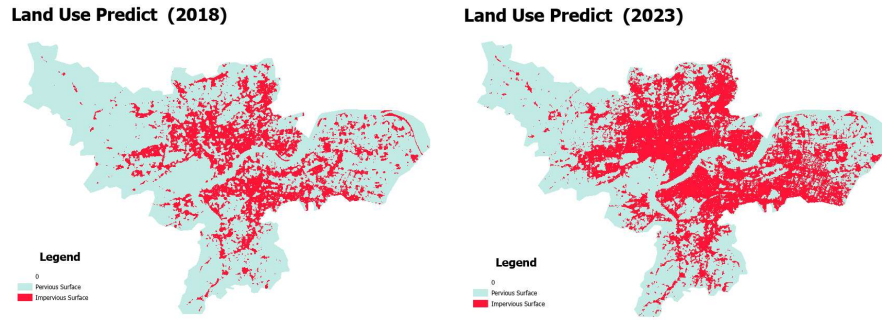


Figure 4: Predict 2018 and 2023 Impervious Surface

2.2 Detect Inundation Area Using HAND Model

To assess flood risk, the Height Above Nearest Drainage (HAND) model was applied using DEM data from the National Remote Sensing Center of China⁴. Flow accumulation was computed and adjusted using 2023 impervious surface data via the formula:

$$\text{adjusted_accumulation} = \text{accumulation} \times (1 + \text{impervious_percent}).$$

Different land covers were assigned runoff coefficients based on guidelines from the U.S. Army Corps of Engineers⁵: water bodies (1.0), urban surfaces (0.6), and natural surfaces (0.0). This adjustment accounts for surface runoff variability, enhancing the HAND model's accuracy under urban conditions. The HAND values represent relative elevation to the nearest drainage path: lower values indicate higher flood susceptibility.

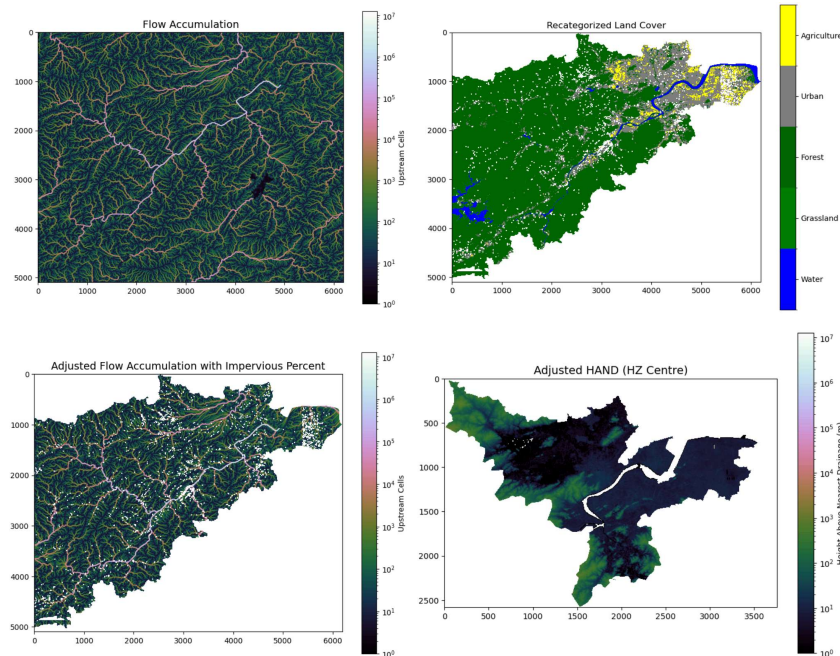


Figure 5: Detect Inundation Area Using HAND Model

⁴ National Remote Sensing Center of China. (2024). Digital elevation model (DEM). GSCloud. <https://www.gscloud.cn/search>

⁵ U.S. Army Corps of Engineers. (2023). Creating land cover, Manning's n values, and impervious layers.

<https://www.hec.usace.army.mil/confluence/rasdocs/r2dum/6.0/developing-a-terrain-model-and-geospatial-layers/creating-land-cover-mannings-n-values-and-impervious-layers>

To further focus to potential inundation areas, HAND threshold values were applied to classify inundation risk zones. These thresholds represent varying degrees of susceptibility to flooding, with lower thresholds capturing areas most prone to inundation due to their proximity in elevation to drainage channels. The spatial distribution of inundation areas under different HAND thresholds reveals distinct patterns. At the 5-meter threshold, inundation zones are primarily concentrated along the Qiantang River, indicating high flood susceptibility in river-adjacent areas. Another cluster in the northwest becomes visible even at this low threshold, reflecting naturally low-lying inland areas. When the threshold is raised to 10 meters, these clusters expand significantly both northwest of the city and along the river, identifying broader areas of flood risk. At the 15-meter threshold, inundation-prone areas extend further, indicating that even relatively flat eastern areas may experience surface water accumulation under extreme rainfall. Based on this comparison, the 10-meter HAND threshold was selected for final analysis as it captures both critical flood-prone zones and balances spatial coverage without overgeneralization.

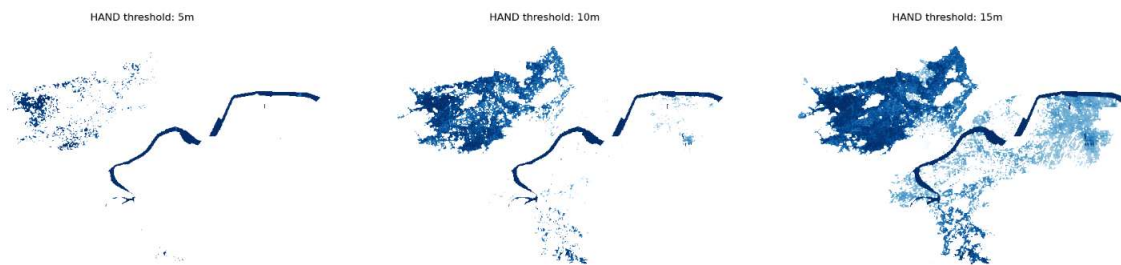


Figure 6: Inundation Area with Different Threshold

2.3 Normalize and Spatial Aggregate

To ensure consistent spatial comparison, a standardized hexagonal grid with 150 per row was established across the study area. Within each unit, impervious surface percentages for 2018 and 2023 and maximum and mean HAND values were calculated. This unified spatial framework enabled the identification of high-risk zones requiring further intervention.

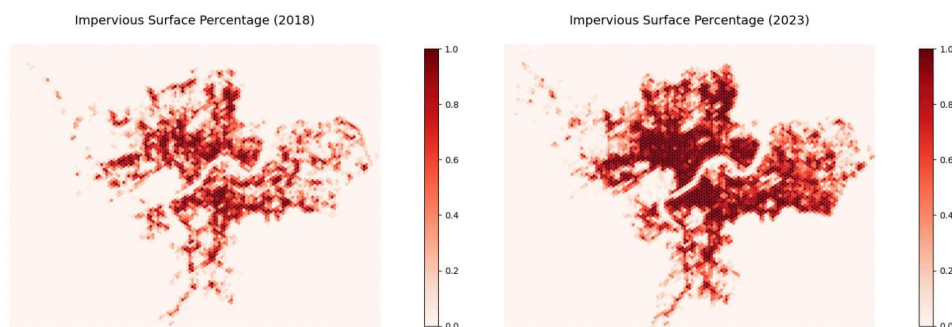


Figure 7-1: Hexagonal Grid (Impervious Surface)

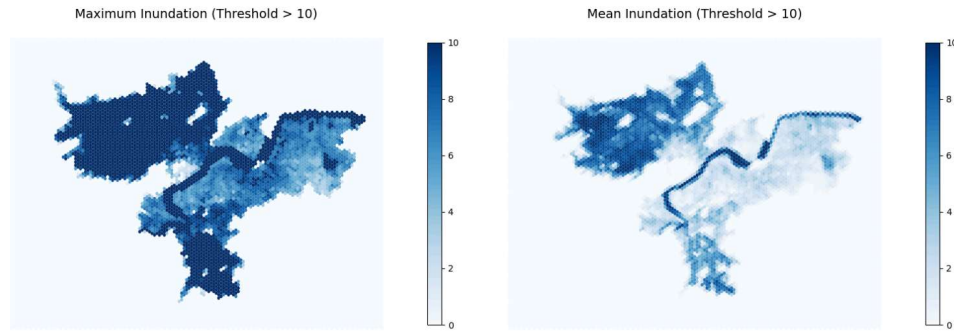


Figure 7-2: Hexagonal Grid (Inundation)

3. Results

Flood risk zones were classified into three levels by integrating impervious surface coverage and HAND values. As shown in Figure 8, units marked in red indicate extreme risk zones, those units with over 50% impervious surface and maximum HAND values greater than 9. In 2018, such areas were clustered in central urban regions, particularly around high-density neighborhoods in north Gongshu and Xihu District. There are also some distributions in southern Xiaoshan District and along Qiantang River. By 2023, these red zones expanded significantly, especially along the Qiantang River corridor and toward the northwestern and southern edges of the built-up area, mainly in Yuhang District, suggesting increased exposure to deep and rapid inundation as urbanization intensified. Chronic risk units in blue, represent units with over 50% impervious surface and mean HAND values above 1. These areas are less susceptible to severe, short-term flooding but face recurring, moderate inundation risks. From 2018 to 2023, these zones have become denser and more spatially continuous, forming a belt particularly in the east, where urban expansion has outpaced drainage improvements. Overall, the shift between 2018 and 2023 indicates a marked increase in both the number and extent of high-risk zones, underlining the spatial correlation between rapid urban development and rising flood vulnerability. These findings highlight the need for differentiated planning responses: targeted mitigation in extreme risk zones, long-term adaptation in chronic risk areas, and proactive green infrastructure integration in low-risk zones to prevent future degradation.

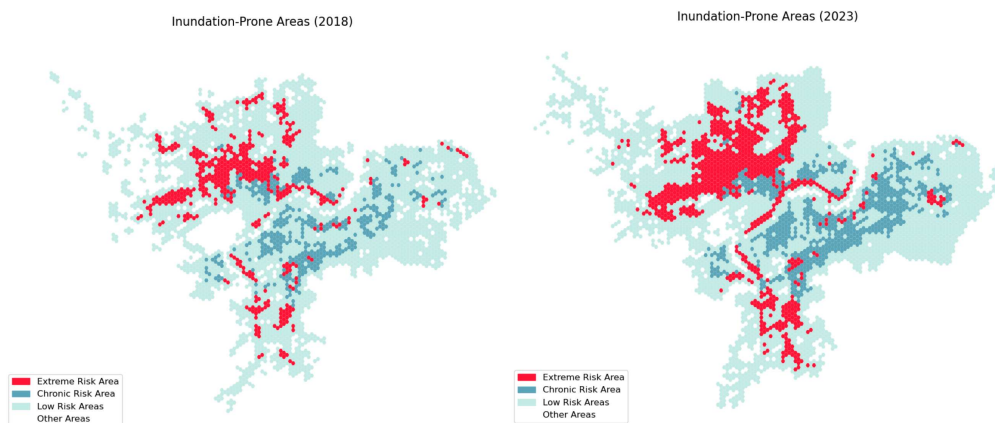


Figure 8 : Inundation Risk in 2018 and 2023

To further visualize urbanization impacts, areas with more than 30% increase in impervious surfaces were mapped and overlaid with flood risk indicators. The results indicate that major urban growth occurred along the northwestern and southeastern edges of the city, corresponding to Yuhang and Xiaoshan Districts respectively, both areas targeted for industrial and logistical development in recent planning strategies. In Yuhang District, the expansion is characterized by large contiguous patches of impervious surface coupled with high HAND-based inundation indices, suggesting that these newly developed areas are at high risk of deep and rapid flooding. This indicates an urgent need to assess whether adequate green and grey stormwater infrastructure has been implemented to mitigate such risks. In contrast, although Xiaoshan District also experienced significant urban growth, the corresponding flood risk levels are generally lower, suggesting either better site selection or more effective flood mitigation measures in place.

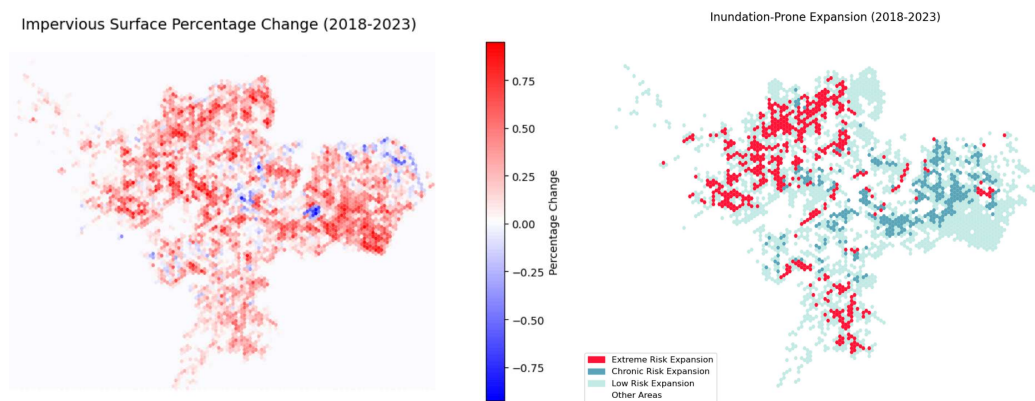


Figure 9 : Impervious Change and Inundation Risk in 5 years

4. Conclusion

The findings of this study underscore the complex interplay between urban land-use change and hydrological risk. The expansion of impervious surfaces in Hangzhou's central districts, especially Yuhang and Xiaoshan, has significantly increased surface runoff, which the adjusted HAND model effectively captures. The spatial aggregation analysis shows that high flood risk zones are not evenly distributed but are spatially clustered in newly developed or rapidly urbanizing fringes that often lack sufficient stormwater infrastructure. This suggests that urban planning in Hangzhou has not kept pace with the hydrological consequences of land conversion. The emergence of "chronic risk zones", areas with moderate but persistent inundation risk, also indicates potential challenges in maintenance and performance of existing drainage systems. A critical implication is the need to integrate green infrastructure including wetlands, permeable pavements, and urban forests into development plans, particularly in areas flagged as emerging hotspots. Urban policies should prioritize both grey infrastructure and nature-based solutions to reduce surface runoff.

Reference:

Darabi, H., et al. (2020). Urban flood risk mapping using data-driven geospatial techniques for a flood-prone case area in Iran. *Hydrology Research*, 51(1), 127–141.
<https://doi.org/10.2166/nh.2019.090>

European Space Agency. (2024). Copernicus Sentinel-2 Level-2A surface reflectance product. Google Earth Engine.
https://developers.google.com/earth-engine/datasets/catalog/COPERNICUS_S2_SR

Jafarpour Ghalehtimouri, K., Che Ros, F., & Rambat, S. (2024). Flood risk assessment through rapid urbanization LULC change with destruction of urban green infrastructures based on NASA Landsat time series data: A case study of Kuala Lumpur between 1990–2021. *Ecological Frontiers*, 44(2), 289–306.
<https://doi.org/10.1016/j.chnaes.2023.06.007>

Li, L., Uyttenhove, P., & Van Eetvelde, V. (2020). Planning green infrastructure to mitigate urban surface water flooding risk – A methodology to identify priority areas applied in the city of Ghent. *Landscape and Urban Planning*, 194, 103703.
<https://doi.org/10.1016/j.landurbplan.2019.103703>

National Remote Sensing Center of China. (2024). Digital elevation model (DEM). GSCloud.
<https://www.gscloud.cn/search>

TianDiTu. (2024). Administrative division boundary data. TianDiTu Cloud Center.
<https://cloudcenter.tianditu.gov.cn/administrativeDivision>

U.S. Army Corps of Engineers. (2023). Creating land cover, Manning's n values, and impervious layers.
<https://www.hec.usace.army.mil/confluence/rasdocs/r2dum/6.0/developing-a-terrain-model-and-geospatial-layers/creating-land-cover-mannings-n-values-and-impervious-layers>

Zhuohong Li, et al. (2023). SinoLC-1: A high-resolution (1 m) national-scale land cover product [Dataset]. Zenodo. <https://doi.org/10.5281/zenodo.7709370>